

Experimental-numerical analyses of the seismic behaviour of cross-laminated wall systems



I. Gavric, G. Rinaldin & C. Amadio

University of Trieste, Italy

M. Fragiaco

University of Sassari, Italy

A. Ceccotti

CNR IVALSA Trees and Timber Institute, S. Michele all'Adige, Italy

SUMMARY:

The paper discusses experimental and numerical seismic analyses of typical connections and wall systems used in cross-laminated (X-Lam) timber buildings. An extended experimental programme on typical X-Lam connections was performed at IVALSA Trees and Timber Institute. In addition, cyclic tests were also carried out on full-scale single and coupled X-Lam wall panels with different configurations and mechanical connectors subjected to lateral force. An advanced non-linear hysteretic spring to describe accurately the cyclic behaviour of connections was implemented in ABAQUS finite element software package as an external subroutine. The FE model with the springs calibrated on single connection tests was then used to reproduce numerically the behaviour of X-Lam wall panels, and the results were compared with the outcomes of experimental full-scale tests carried out at IVALSA. The developed model is suitable for evaluating dissipated energy and seismic vulnerability of X-Lam structures.

Keywords: Experimental tests, Components approach, Connections, X-Lam wall systems, Numerical analysis

1. INTRODUCTION

This paper presents some of the results of an extensive experimental programme on typical X-Lam connections and X-Lam wall panels, conducted at CNR-IVALSA research institute, and compares some of the experimental results with numerical predictions using an advanced numerical model. The goal of this research is to provide a better insight of the seismic performance of connections in cross-laminated timber buildings subjected to seismic actions. A new component model for cyclic (seismic) analysis of cross-laminated (X-Lam) timber buildings was developed at the University of Trieste (Rinaldin et al. 2011). X-Lam panels are schematized with linear-elastic shell elements with a composite section made of orthotropic layers, while the steel connections are modelled using non-linear springs with hysteretic behaviour. The model is based on the evidence that energy dissipation of X-Lam wooden buildings subjected to earthquake excitation mainly occurs in the metal connections between panels and with the foundations. The advantage of the proposed model is the possibility to calibrate each spring on the basis of cyclic tests carried out on different types of connection, with the possibility to predict the cyclic behaviour of entire panels, subassemblies, and buildings. A phenomenological way to represent the non-linear hysteretic behaviour has been chosen, since it allows the user to fully control and model the metal connections in a simple way. In particular, the model includes allowance for stiffness and strength degradation, which are features of great importance in the cyclic behaviour of timber structures. All the phenomenological relationships discussed in the paper were based on the results of force vs. displacement cyclic experimental data currently available.

2. COMPONENT APPROACH

A components approach has been used to model X-Lam walls and wall systems, with the aim to predict the cyclic (seismic) behaviour with good accuracy. In this approach, each connector (angle

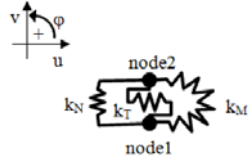
bracket, hold-down, self-tapping screws) is schematized with a non-linear spring characterized by a hysteretic behaviour. The model has been implemented in a widespread software package such as Abaqus using an external user subroutine written in Fortran.

2.1. Constitutive model of the components

Each metal connection (component) has been modelled as a non-linear spring with hysteretic behaviour. The actual curves have been approximated with piecewise linear laws, more specifically tri-linear curves, which have been parameterized to allow the user to fully control their shape. Three different types of curve have been developed: for angle brackets, for screws and for hold-downs. Each curve is made of several branches composing the backbone curve and the hysteretic cycle.

The non-linear spring connects two coincident points in the undeformed state, hence it has zero length. In the most general case, every spring returns to the solver the three forces that develop in its plane and the corresponding three stiffnesses (see Table 2.1). Although only planar springs with three degrees of freedom have been considered in this study for the sake of simplicity as this is the most important case, the theory can be easily generalized to the case of a spatial spring with six degrees of freedom.

Table 2.1. Basic definition of non-linear springs

 <p>Schematic of springs</p>	<p>Congruence equations – Spring degrees of freedom:</p> $\varphi = \varphi_2 - \varphi_1$ $\gamma = u_2 - u_1$ $\varepsilon = v_2 - v_1$
<p>Constitutive equations – Spring forces:</p> $M = M(\varphi)$ $T = T(\gamma)$ $N = N(\varepsilon)$	<p>Nodal equilibrium equations:</p> $T_1 = T$ $T_2 = -T$ $M_1 = M$ $M_2 = -M$ $N_1 = N$ $N_2 = -N$

2.2. Hysteretic laws

Figure 2.1a displays the shear force vs. shear displacement (slip) piecewise linear law used to model the behaviour of screw and angle bracket connections. The model is defined by 9 independent input parameters and uses 32 state variables per cycle. The input parameters are:

1. Elastic stiffness, k_{el} ;
2. Yielding force, F_y ;
3. First inelastic stiffness (hardening branch), k_{p1} ;
4. Peak strength, F_{max} ;
5. Second inelastic stiffness (softening or hardening branch), k_{p2} ;
6. K_{sc} factor: it sets the unloading stiffness of branches #4 and #50, which is obtained by multiplying the elastic stiffness by this factor K_{sc} ;
7. RC parameter: it sets the lower limit of branches #5 and #40 by multiplying the force value F attained before entering the unloading path by this parameter RC ;
8. SC parameter: it sets the lower limit of branches #4 and #50 by multiplying the force value attained before entering the unloading path F by this parameter SC ;
9. Ultimate displacement, D_u : when this value is attained, a brittle failure occurs.

Figure 2.1b displays the axial force vs. axial displacement piecewise linear relationship used to model the behaviour of the hold-down connector. Same parameters as before were used. Four additional parameters are used to calibrate the strength and stiffness degradation, which are explained in the following Section.

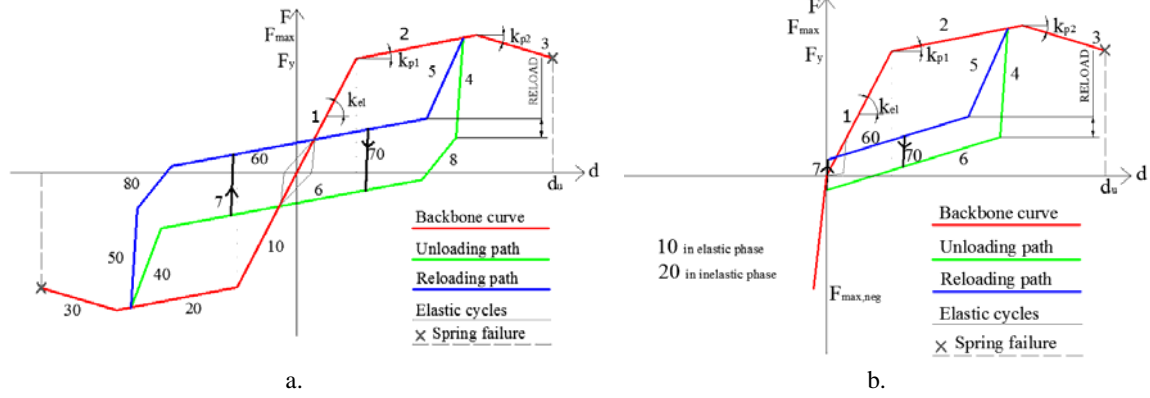


Figure 2.1. Piecewise linear relationship of screws and angle bracket springs (left, a.) and hold-down springs (right, b.)

2.3. Stiffness and strength degradation

Stiffness and strength degradations have been implemented in the model as they are both important features of timber connections. A degradation of stiffness proportional to the maximum displacement attained during the load history has been assumed for the last unloading branches #5 and #50 (after the pinching effect) for both spring models. This effect has been taken into account using Eqn. 2.1:

$$k_{deg} = k_{el} \left[1 - \frac{D_{max}}{D_{ult}} (1 - d_{kf}) \right] \quad (2.1)$$

where:

- k_{deg} = degraded stiffness;
- k_{el} = elastic stiffness;
- D_{max} = maximum displacement attained during the load history;
- D_{ult} = ultimate displacement;
- d_{kf} = stiffness degradation parameter.

The strength degradation depends on the energy dissipated and on the maximum displacement attained during the load history. Due to the complexity of evaluating the dependence of the strength degradation on both these quantities, three calibration parameters have been introduced: a linear and two exponential ones. The adopted relationship is reported in Eqn. 2.2.

$$\Delta d = \gamma \cdot d_{el} \cdot \left(\frac{E_{dis} - E_{dis(A)}}{E_{dis}} \right)^\alpha \cdot \left(\frac{D_{max}}{D_{ult}} \right)^\beta \quad (2.2)$$

where:

- Δd = additional displacement at reloading;
- γ = linear parameter;
- d_{el} = displacement at yielding force;
- α = exponential degradation parameter;
- E_{dis} = dissipated energy;
- $E_{dis(A)}$ = dissipated energy at the beginning of unloading path;
- D_{max} = maximum displacement attained during the loading history;
- D_{ult} = ultimate displacement;
- β = exponential degradation parameter.

2.4. Strength domain and friction effect

A strength domain was implemented for the aforementioned user element. The domain involve shear and axial strength in each connector, and is defined by Eqn. 2.3.

$$\left(\frac{F_N}{R_N}\right)^2 + \left(\frac{F_V}{R_V}\right)^2 \leq 1 \quad (2.3)$$

where:

F_N = axial force at the previous analysis step;

R_N = yielding axial strength given as an input by the user;

F_V = shear force at the previous analysis step;

R_V = yielding shear strength given as an input by the user.

Also the effect of panel-panel or panel-foundation friction can be taken into account through an additional sliding resistance (static friction force), calculated with Eqn. 2.4. The frictional behaviour has not been considered in the examples reported in this paper as it needs to be further investigated.

$$F_f = k_f \cdot F_N \quad (2.4)$$

where:

F_N = axial force at the current analysis step;

k_f = static friction coefficient; F_f = static friction force.

The dynamic friction force is calculated similarly to Eqn. 2.4 by replacing the static friction coefficient k_f with the dynamic friction coefficient k_d .

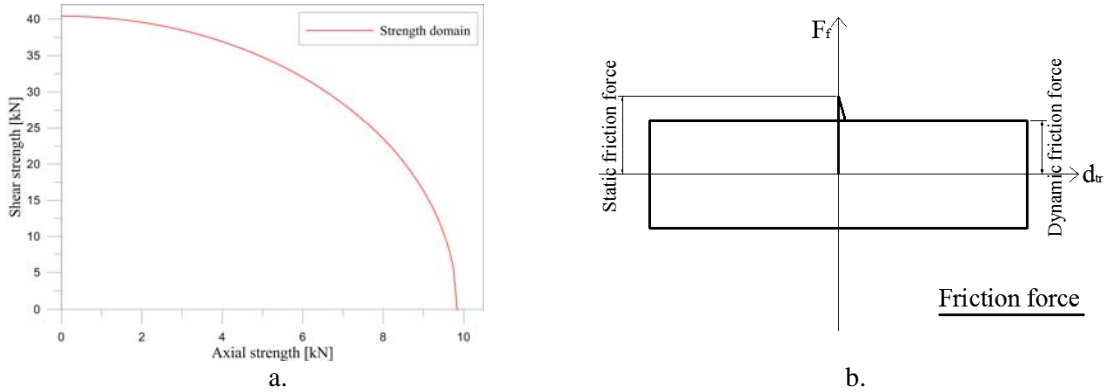


Figure 2.2. Strength domain (left, a.) and friction force at constant axial load (right, b.)

3. EXPERIMENTAL TEST PROGRAMME

An extended experimental programme on typical X-Lam connections was performed at IVALSA Trees and Timber Institute. In addition, cyclic tests were carried out on full-scale single and coupled cross-lam wall panels with different configurations and mechanical connectors subjected to lateral force (Gavric et al. 2011). In this paper, some of the results and analyses from the experimental tests are presented.

3.1. Connection tests

In order to obtain statistically reliable values to be used for analytical and numerical analyses, at least one monotonic and six cyclic tests were performed for each of the twenty different configurations of typical X-Lam connections, with an addition of three to five tests for each configuration with changed

connection layout. More than 200 tests were performed in total, following the EN12512 (2001) standard. Shear and pull-out monotonic and cyclic tests were carried out on hold-downs (Fig. 3.1.a) and steel angle connectors (Fig. 3.1.b) used to anchor the wall panels to foundation and to connect wall panels to floor panels in the upper stories (Gavric et al. 2011). In-plane shear tests were also performed on mechanical screwed connections between adjacent X-Lam panels, using different types of vertical joints. In addition, cyclic tests were carried out also on orthogonally connected panels (wall-wall and wall-floor) subjected to shear and withdrawal load (Gavric et al. 2012). The hold-downs used in the tests were type WHT540 with 12 annular ringed nails 4x60 mm, type Anker (Fig. 3.1.a). This relatively new type of hold-down matches well with the geometry and thickness of the older type HTT22 of hold-down, originally used in SOFIE project. The type of angle bracket used was the BMF 90x116x48x3 mm with 11 annular ringed nails 4x60 mm, type Anker (Fig. 3.1.b). Two different types of in-plane screwed connections between adjacent walls were tested: (i) the so-called ‘over-lap’ joint, with 50 mm overlap length; and (ii) a spline joint with 28 mm thick and 180 mm wide LVL strip. Both of them were screwed with self-tapping screws type HBS $\phi 8 \times 80$ mm.



Figure 3.1. Experimental setup of hold-down loaded in tension (left a.); angle bracket loaded in shear (right b.)

3.2. Wall tests

In addition to the monotonic and cyclic test programme conducted at CNR-IVALSA in 2005 (Ceccotti et al. 2006), a series of cyclic tests were also carried out on full-scale single and coupled X-Lam wall panels with different configurations and mechanical connectors subjected to lateral force. The aim of these additional experimental tests on wall panels is to find out the differences in seismic behaviour between long single walls and a series of adjacent wall panels with vertically screwed joints. Detailed investigation of energy dissipation properties and damping capacity were done.



Figure 3.2. Experimental setup of full-scale X-Lam wall panels subjected to horizontal load - single wall (left, a.) and coupled wall with LVL spline vertical joint (right, b.)

4. EXPERIMENTAL-NUMERICAL ANALYSES

4.1. Spring calibration

Each type of spring was calibrated on the experimental results reported in (Gavric et al. 2011). The calibration was done by following the steps listed herein after:

1. the yielding and peak force were extracted from the experimental results;
2. the elastic stiffness was estimated once a good fit of the yielding displacement was obtained;
3. the hardening stiffness of the plastic branch was chosen on the basis of the backbone curve;
4. other parameters, such as the stiffness and the strength degradation factors, were evaluated in an iterative way until a good fit between the experimental curve and the model was obtained.

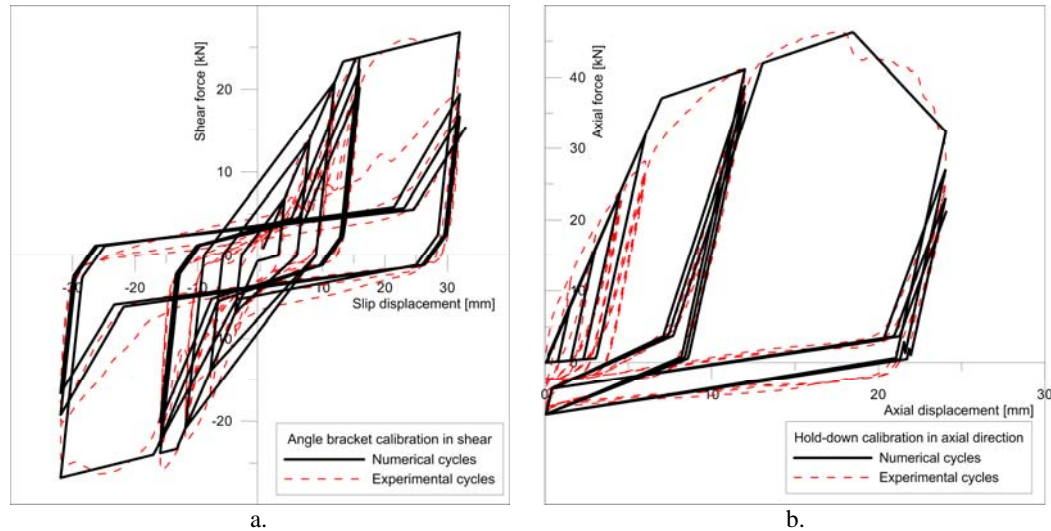


Figure 4.1. Calibration of angle bracket springs (left, a.) and calibration of hold-down springs (right, b.)

Table 4.1. Calibration of mean values obtained from experimental results on X-Lam connections

Parameter description	Angle bracket: shear	Angle bracket: tension	Hold-down: tension	Hold-down: shear	Screws (half-lap joint): vert. shear	Screws (half-lap joint): hor. shear	Screws (spline joint): vert. shear	Screws (spline joint): hor. shear
Elastic stiff. k_{el} [kN/m]	1.78	2.76	4.82	0.99	1.67	1.85	0.9	1.14
1st inel. stiff. k_{p1} [kN/m]	0.22	0.41	0.69	0.12	0.13	0.18	0.094	0.09
2nd inel. stiff. k_{p2} [kN/m]	-0.9	-0.86	-0.96	-0.8	-0.08	-0.07	-0.26	-0.27
Yiel. force F_y [kN]	23.77	19.23	40.3	9.79	2.54	2.79	4.81	3.24
Max. force F_{max} [kN]	27.71	23.51	48.33	13.88	5.51	5.3	7.56	6.51
Unload. ratio SC [%]	0.86	0.99	0.95	0.88	0.93	0.85	0.95	0.75
Reload. ratio RC [%]	0.66	0.88	0.86	0.66	0.78	0.73	0.85	0.61
Ult. displ. D_u [mm]	64	24	30.2	48	40	32	40	40.4

To speed up the calibration process, the software So.ph.i. (acronym for SOftware for PHenomenological Implementations) has been developed using the Visual Basic .NET language (MSDN 2011). So.ph.i. (2002) allows the user to visualize the results of the calibration made upon an experimental data set of a certain spring component. In addition, So.ph.i releases an input data file in the right format that will be used in the user subroutine implemented in Abaqus for cyclic modelling of the corresponding spring component. An automated calibration procedure based on EN 12512:2001 has been implemented in So.ph.i. This allows the user to obtain automatically elastic stiffness and yielding force values according to the code. In Table 4.1 the mean characteristics of single spring components calculated from the tests presented in (Gavric et al. 2011) is shown. These values have been used in all subsequent analyses. The comparison between experimental and model curves is displayed in Fig. 4.1 for angle bracket in shear and hold-down subjected to axial force.

4.2. Numerical analyses

Once calibrated, the hold-down and angle bracket spring components were used to model full-scale crosslam panels tested at CNR-IVALSA. In the case of single wall panels, two experimental tests were analysed. The first panel (Test 1.1) was connected to the foundation with two angle brackets and two hold-downs at both ends. Hold-downs were type HTT22 with 12 nails $\phi 4 \times 60 \text{mm}$ anchored with $\phi 16$ bolts and angle brackets were type BMF 90x48x3x116mm with 11 nails $\phi 4 \times 60 \text{mm}$ anchored to the foundation with $\phi 12$ bolts. The second panel (Test 1.2) was anchored with the same type of connectors and the same number of fasteners, except the number of angle bracket that in this case was four instead of two. The wall panel was in both cases 5-layered, with each layer 17mm thick, and with a total thickness of 85 mm. Panel dimensions were 2.95x2.95m. The loading protocol followed during the tests was the one prescribed by EN12512 (EN12512 2001). The vertical load applied on the top of the specimens was 18.5kN/m. The X-Lam wall was modelled with elastic shell elements, whilst every connection was modelled with hysteretic non-linear springs, placed as in Figure 4.2, calibrated on the experimental results as displayed in Fig. 4.1.

The experimental-numerical comparison is displayed in Figure 4.3 as lateral force vs. top floor deflection, showing an overall acceptable approximation. It must also be pointed out that, unlike other software packages, no convergence problems arose at any time during the cyclic analysis carried out with the proposed model.

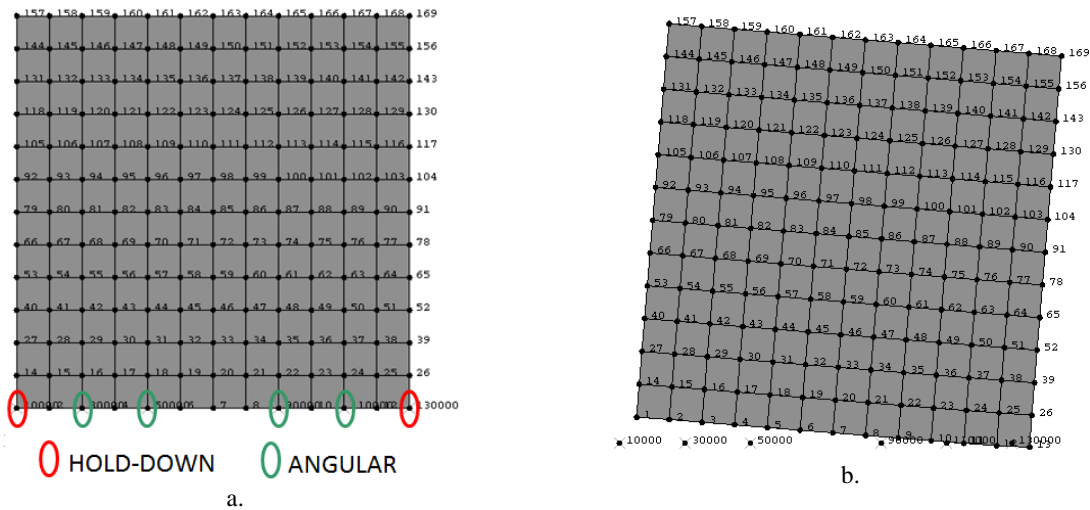


Figure 4.2. Mesh and springs used to model the Panel 1.2. (left ,a.) and an example of deformed shape predicted in the numerical analysis (right, b.)

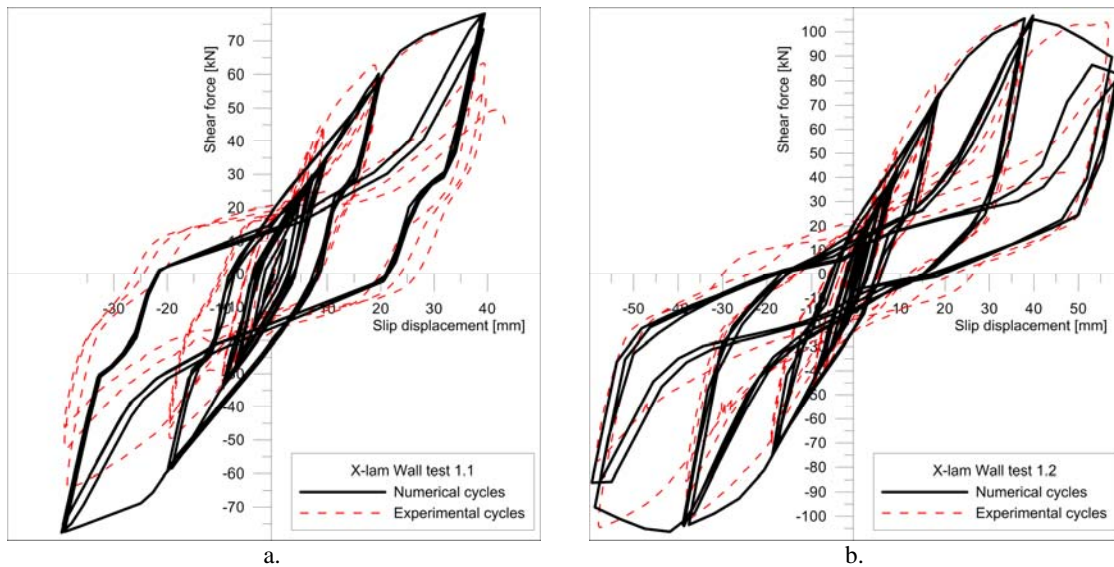


Figure 4.3. Numerical-experimental comparison on cyclic behaviour of X-Lam panel 1.1 (left, a.) and panel 1.2 (right b.)

The coupled walls had the same layout, size and type of connectors used to anchor each wall panel to the foundation as the single wall 1.2. Two types of vertical joint between adjacent panels were investigated: (i) in Test 2.1, a half-lap joint with self-threaded screws type HBS $\phi 8 \times 80 \text{mm}$ were used to connect the panels together, and the screws were placed on a single row at 150mm c/c; and (ii) in Test 3.1, a spline joint with LVL strip and double row of self-threaded screws at 150 mm c/c was used. Additional springs representing the screws hysteretic behaviour were used at the wall-wall interface. These spring elements, placed along the vertical symmetry axis of the joint, connect the two adjacent panels. Numerical-experimental comparisons of total lateral force vs. top deflection of wall tests 2.1 and 3.1 are presented in Figure 4.4.

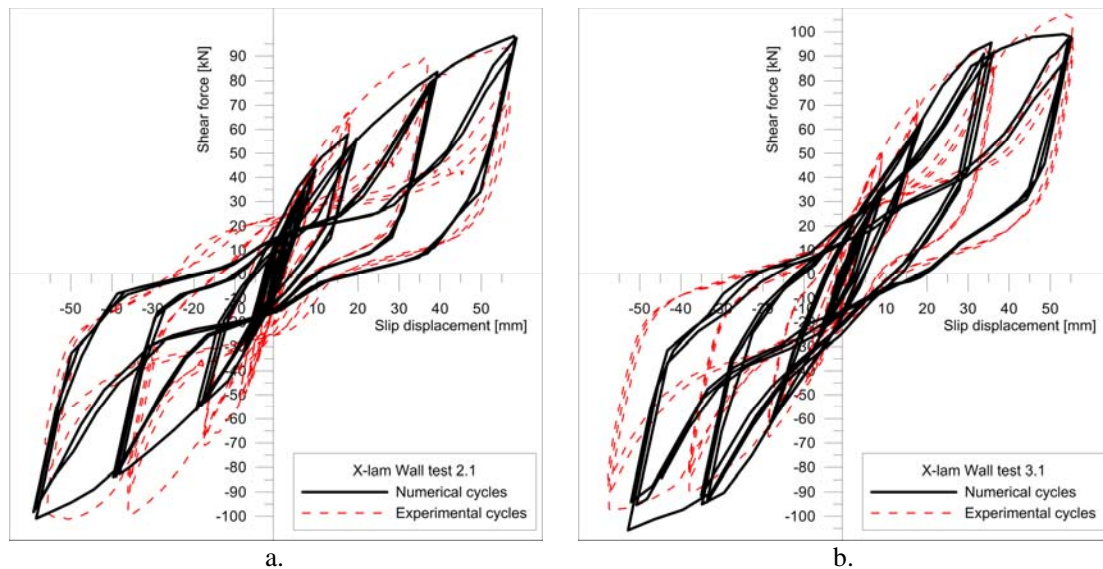


Figure 4.4. Numerical-experimental comparison on cyclic behaviour of X-Lam panel 2.1 (left, a.) and 3.1 (right, b.)

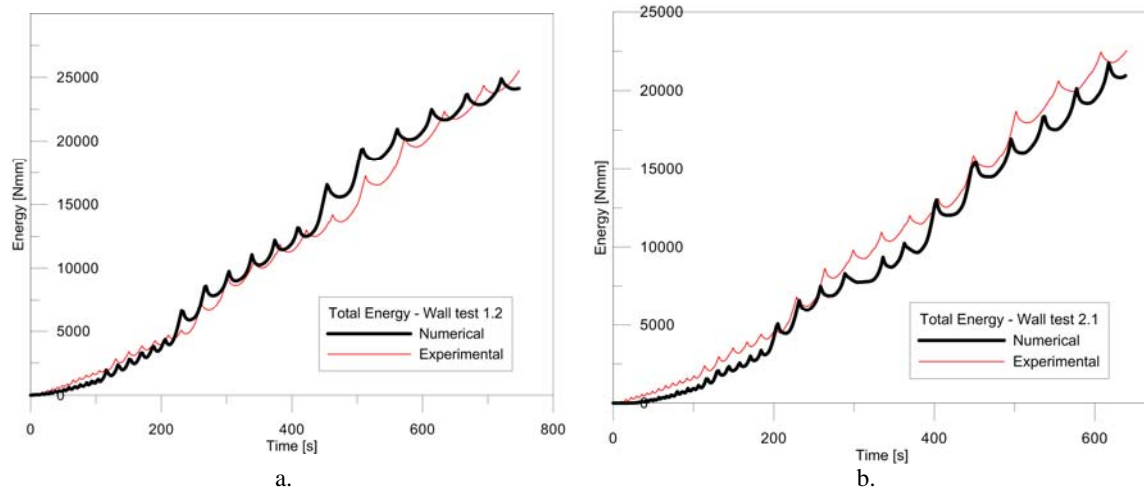


Figure 4.5. Numerical-experimental comparison of time-history of the total dissipated energy during the cyclic tests on X-Lam panel 1.2 (left, a.) and 2.1 (right, b.)

During the experimental tests, a non-symmetrical behaviour was noticed, while the proposed numerical approach returns symmetrical results. Despite this fact, there is an acceptable accuracy between experimental and numerical curves; therefore, it is possible to use the presented model to investigate the behaviour of other structures having similar characteristics in terms of connection and wood properties. Furthermore, different types of wall configuration and layout can be analysed with a proper calibration of the spring elements over the experimental properties of connectors.

Also the numerical total energies were computed and compared with the experimental ones, showing a difference of 3.6% on average; this is a further confirmation of the model accuracy as the dissipated energy is a fundamental quantity in seismic analyses.

5. CONCLUSIONS

Several configurations of typical X-Lam connections and wall panels were investigated by means of cyclic tests, carried out according to EN12512 standard. Wall configurations included different anchoring systems, single and coupled walls, and different types of screws to connect the panels.

A component approach for non-linear dynamic analysis of structures made from cross-laminated solid timber was presented in this paper. A non-linear spring for every type of connectors has been modelled in a phenomenological way. Based on experimental evidence, all energy dissipation was assumed to take place in the steel connectors, whilst the timber panel was regarded as linear elastic. Two different hysteretic loops characterized by a tri-linear backbone curve with significant pinching effect were implemented in Abaqus software package using external user-subroutines. Allowance for strength and stiffness degradation, based on the dissipated energy and maximum displacement attained, was also made. Such hysteretic laws were then fitted with the experimental results available for hold-downs, angle brackets, and screwed connection. A program was also developed to make the calibration of the hysteretic law on the experimental results easier. After calibration, the non-linear spring components were used to model cyclic tests carried out at CNR-IVALSA on full-scale single and coupled cross-lam panels, showing an overall acceptable accuracy in terms of both lateral displacement and dissipated energy. The numerical analyses in comparison with the experimental results have confirmed that the layout and design of the joints is critical for the overall behaviour of the X-Lam structural system.

The proposed hysteretic model is very robust and unlike other software packages does not suffer from convergence problem. As such, it could be used to model the seismic performance of cross-laminated buildings and subassemblies. The cyclic behaviour of the steel connectors allows a correct estimation

of the dissipated energy and, consequently, a reliable prediction of the seismic capacity of the whole timber building. The model will be used, in particular, to: (i) fully understand the experimental results of the full-scale 3-storey and 7-storey crosslam buildings tested on a shaking table in Japan (Ceccotti 2008, Progettosofie 2008); (ii) extend the experimental results to different building configurations including non-residential destinations; and (iii) investigate the behaviour factors of multi-storey cross-lam timber buildings.

AKNOWLEDGEMENT

The experimental research presented in this paper was funded by the Autonomous Province of Trento (Italy) within the SOFIE research project. The authors would like to acknowledge the contribution to this research of IVALSA laboratory staff Mario Pinna, Diego Magnago and Paolo Dellantonio, who provided technical expertise for the experimental testing.

REFERENCES

- Ceccotti, A., Lauriola, M., Pinna, M., Sandhaas, C. (2006). SOFIE Project - Cyclic Tests on Cross-Laminated Wooden Panels. *Proceedings of the 9th World conference on timber engineering*, August 6-August 10, Portland, Oregon, USA.
- Ceccotti, A. (2008). New technologies for Construction of Medium-Rise buildings in Seismic Regions: The XLAM case. *Journal of the International Association for Bridge and Structural Engineering*. Vol 2:2008, 156-165.
- EN12512 (2001). Timber structures - Test methods - Cyclic testing of joints made with mechanical fasteners. CEN, Brussels, Belgium.
- Gavric, I., Ceccotti, A., Fragiaco, M. (2011). Experimental cyclic tests on cross-laminated timber panels and typical connections. *Proceedings of the 14th ANIDIS Conference*, Bari (Italy), September 18th-22nd, DVD.
- Gavric, I., Fragiaco, M. and Ceccotti, A. (2012). Strength and deformation characteristics of typical X-Lam connections. *12th World conference on timber engineering*, Auckland, New Zealand. (submitted)
- MSDN - Microsoft Developer Network (2011). <http://msdn.microsoft.com>. Internet site.
- Progettosofie (2008) - <http://www.progettosofie.it/> - new architecture with wood. Internet site.
- Rinaldin, G., Amadio, C., Fragiaco, M. (2011). A component approach for non-linear behaviour of cross-laminated solid timber panels. *Proceedings of the 14th ANIDIS Conference*, Bari (Italy), September 18th-22nd, DVD.
- So.ph.i. Software (2012). <http://giovanni.rinaldin.org/>. Internet site